DOI:
10.1016/j.niox.2018.06.001

Document Version
Peer reviewed version

Accepted Manuscript

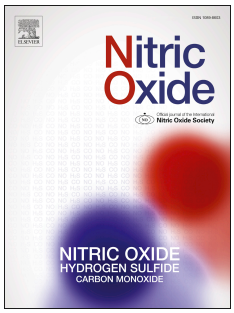

Inducible nitric oxide synthase-mediated injury in a mouse model of acute salivary gland dysfunction

Abeer Shaalan, Guy Carpenter, Gordon Proctor

PII: S1089-8603(18)30016-8

DOI: 10.1016/j.niox.2018.06.001

Reference: YNIOX 1797

To appear in: *Nitric Oxide*

Received Date: 16 January 2018

Revised Date: 31 May 2018

Accepted Date: 4 June 2018

Please cite this article as: A. Shaalan, G. Carpenter, G. Proctor, Inducible nitric oxide synthase-mediated injury in a mouse model of acute salivary gland dysfunction, *Nitric Oxide* (2018), doi: 10.1016/j.niox.2018.06.001.

Title: Inducible Nitric Oxide Synthase-Mediated Injury in a Mouse Model of Acute Salivary Gland Dysfunction

Authors: Abeer Shaalan[1,2], Guy Carpenter[1] and Gordon Proctor[1]

[1] Mucosal and Salivary Biology, Dental Institute, King's College London, United Kingdom

[2] Corresponding author: Abeer Shaalan, Floor 17 Tower Wing, King's College London, Dental Institute, Guy's & St Thomas' Hospitals, Great Maze Pond, London, SE1 9RT, abeer.shaalan@kcl.ac.uk**.**

Abstract

Aim: Inducible nitric oxide synthase (iNOS) is a key regulator of the innate immune system. The aim of the current study was to explore whether innate immune-mediated iNOS and reactive nitrogen species acutely perturb acinar cell physiology and calcium homeostasis of exocrine salivary tissues.

Methods: Innate immunity in the submandibular gland of C57BL/6 mice was locally activated via intraductal retrograde infusion of polyinosinic:polycytidylic acid (poly (I:C). Expressions of iNOS and the activity of the reactive nitrogen species peroxynitrite, were evaluated by immunohistochemistry. Mice were pre-treated with the selective iNOS inhibitor aminoguanidine in order to substantiate the injurious effect of the nitrosative signal on the key calcium regulator sarcoplasmic/endoplasmic reticulum calcium ATPase (SERCA2b) and calcium signalling.

Results: Challenging salivary gland innate immunity with poly (I:C) prompted upregulated expression of iNOS and the generation of peroxynitrite. Inhibition of iNOS/peroxynitrite revealed the role played by upregulated nitrosative signalling in: dysregulated expression of SERCA2b, perturbed calcium homeostasis and loss of saliva secretion.

Conclusion: iNOS mediates disruption of exocrine calcium signalling causing secretory dysfunction following activation of innate immunity in a novel salivary gland injury model.

Keywords: 3-Nitrotyrosine; calcium; inducible nitric oxide synthase; innate immunity; salivary gland; SERCA2b.

1. Introduction

Saliva performs a number of important functions that are essential for the maintenance of oral health [1]. The key trigger for saliva secretion is initiated by parasympathetic nerve mediated stimuli and by the action of acetylcholine on acinar cell muscarinic receptors inducing an increase in intracellular calcium $[Ca^{2+}]_i$ [2]. Increased acinar cell $[Ca^{2+}]_i$ leads to regulation of ion channel activities, secretion of electrolyte and generation of the appropriate osmotic gradient required to drive fluid secretion [3]. Termination of the autonomimetic signal requires pumping out of calcium by plasma-membrane-Ca^{2+}-activated-ATPase, or PMCA [4] and Ca^{2+} re-uptake into the endoplasmic reticulum by the sarco-endoplasmic-reticulum-Ca^{2+}-activated ATPase, or SERCA [5; 6].

The most severe forms of long-lasting, irreversible dry mouth are seen in patients exposed to irradiation therapy of the head and neck and patients with the autoimmune disease Sjögren's syndrome [1]. Loss of saliva production in these patients severely affects their quality of life due to difficult with swallowing, rampant dental caries, oral mucosal lesions and fungal infections. The latest advances in elucidating the pathogenesis of primary Sjögren's syndrome suggest that innate immune dysregulation drives the disease, with patients experiencing salivary hypofunction [7; 8] as well as aberrant Ca^{2+} signalling [3; 9]. However, the molecular links between these proposed mechanisms have not been previously elucidated.

Inducible nitric oxide synthase (iNOS) is an inflammatory mediator, the expression of which is increased by a wide range of stimuli, such as microbial products and cytokines [10]. In contrast to the constitutive NOS isoforms (NOS1 or nNOS, produced by neurons; NOS3 or eNOS, produced by endothelial cells), which produce nitric oxide (NO) within seconds, with direct and short acting activities, iNOS produces very large, toxic amounts of NO in a sustained manner [11]. In addition, NO and superoxide formed during the inflammatory response react, yielding peroxynitrite (ONOO-) anion, which is a potent oxidant and nitrating agent [12]. iNOS-derived NO and ONOO- have been implicated as potential mediators of exocrine gland damage in murine models of Sjögren's syndrome [13] and irradiation [14] and studies *in vitro* have indicated that nitric oxide donors can interfere wth acinar cell calcium signalling (Smith & Dawson) . However, the early physiologic responses of the SGs to acute iNOS and ONOO- induction have not been previously investigated.

In a previous study, the innate immune stimulant poly (I:C) prompted TLR3-mediated SMG injury and loss of function, which paralleled extensive upregulation of acinar iNOS [15]. Aminoguanidine (AG), a selective inhibitor of iNOS, is a phenylhydrazine compound which has many biological effects with nontoxic function

[16]. In the present work, mice were pre-treated with AG to investigate the underlying mechanisms through which acute nitrosative stress signals can disrupt the SG physiology.

2. Materials and Methods

2.1 Mice

Female C57BL/6 mice weighing 18-21 grams (Harlan Labs Ltd., Loughborough, UK) and aged 10-12 weeks were housed in a temperature-controlled environment under a 12 h light–dark cycle, with free access to food and water. All procedures were approved by the local ethics committee and performed under general anaesthesia under a Home Office license.

2.2 Poly (I:C) injury model and assessment of secretion

The C57BL/6 mouse SMGs were cannulated as previously described [17]. For recovery experiments, mice were anaesthetised intraperitoneally (i.p.) with 0.1 ml of combined 5 mg Ketamine/1 mg Xylazine. Briefly, poly (I:C) (P1530-25MG, Sigma-Aldrich) was diluted in saline (4mg/ml) and pre-mixed with Trypan blue (T8154-100ML-Sigma- Aldrich). Eighty micrograms of poly (I:C) in 20 µls were loaded into a 0.3 ml syringe (6134900, VWR International), attached to a glass cannula (Supelco, 25715, PA- USA) which was inserted into Wharton's duct under a stereomicroscope. Poly (I:C) was injected slowly and constantly into the left SMG. The same volume of the vehicle was delivered to the right SMG as a contralateral negative control. For functional assessment, mice were anaesthetized with 150µl of Pentobarbital Sodium (Euthatal, Merial) 1 mg/ml (i.p.), followed by endotracheal intubation. SMG ducts were ventrally exposed and cut. Saliva was collected in pre-weighed Eppendorf tubes. Saliva collection proceeded for 5 min following stimulation with pilocarpine (0.5mg/kg i.p.). The volume of saliva was calculated as 1mg = 1µl saliva and results were expressed as µl saliva/min.

2.3 Aminoguanidine (AG) mouse model

For short term inhibition, the selective iNOS Inhibitor; aminoguanidine Hydrochloride, 98+% (Sigma, 396494) was used (100mg/kg i.p. AG and 0.1 mg AG combined with poly (I:C)). For long term inhibition [18]: 2.5% AG in drinking water for 7 days and 0.1 mg AG combined with poly (I:C). While in short term experiments, saliva and tissues were collected after 9 hr of poly (I:C) injection, in long term experiments, sample collection took place after 24h.

2.4 Western Blot

Tissues stored in RNAlater® were retrieved, homogenized in cell lysis buffer (AA-LYS-10 ml- RayBiotech, Inc., Norcross, GA) plus protease inhibitor cocktail (1:10 dilution, Calbiochem, UK) using a FastPrep™ tissue homogenizer (MP Biomedicals Santa Ana, CA). Protein concentration was measured using the Qubit® protein

assay kit (Q33211, Invitrogen™, UK) and Qubit® 3.0 Fluorometer (Q33216, Invitrogen™, UK) and a total of 15 µg /lane of the different lysates were separated by SDS-PAGE on a 4-12% Novex polyacrylamide gel (Invitrogen, UK). Electro-transfer of proteins was done for 1 hour to 0.2 µm pore–size nitrocellulose membrane (1620112, Bio-Rad, UK) according to standard protocol (Invitrogen, UK, Paisley), followed by membrane blocking with 5% bovine serum albumin. Membranes were incubated at 4°C overnight with an antibody to mouse monoclonal 3-nitrtyrosine (3-NT) (Millipore, 05-233, 1:1000) in blocking buffer then washed and incubated with the HRP conjugated anti-mouse secondary antibody in blocking buffer at room temperature for 1 h. For signal development, an Enhanced Chemioluminescence substrate (ECL, GE Healthcare, UK) was prepared following the kit manufacturer's recommendations and applied over the membranes. Positive and negative protein expression was assessed and captured using ChemiDoc™ MP System (Bio-Rad, UK).

2.5 Immunohistochemistry and image analysis

Three µm tissue sections were deparaffinized, rehydrated, and unmasked in a single step using Trilogy™ (Cell Marque, Rocklin, CA, 920P-06). To block endogenous peroxidase activity and non-specific background, sections were incubated in 3% hydrogen peroxide solution for 20-30 minutes. To block all epitopes on the tissue samples and prevent nonspecific antibody binding, sections were incubated with 1% BSA in 1X TBS, pH7.6 for 5 minutes. Primary antibody (Table 1) was applied at the appropriate working dilution overnight at 4°C, followed by secondary antibody (Table 1) for 60 mins at room temperature. Colour was developed for 5 mins in DAB solution (Pierce™ 34002) and slides counterstained in Mayer haematoxylin and DPX-mounted for light microscopy. For semi-quantitative image analysis of SERCA2 immunoexpression, fifteen random high magnification fields (five from three independent experiments) were captured and colour images of 640 × 480 pixel resolution were then analysed by semi-quantitative digitalized image analysis using ImageJ, NIH® [19]. Briefly, images were transformed by threshold mode to locate the positive immunostained area, then converted to 8-bit images in grey scale. Subsequently, the area percentage of SERCA2 positive immunostaining was calculated by the area fraction command within measuring mode which was expressed as the percentage of red pixels/SMG tissue section.

2.6 Confocal microscopy

Fluorescent images were captured on a Leica SP5 confocal microscope with an HCX PL APO CS 40× oil objective.

2.7 Acute Isolation of SMGs and intracellular Ca^{2+} measurement

The protocol that was optimized and implemented to measure changes in intracellular Ca^{2+} concentrations, is detailed in [20]. Changes in resting and stimulated $[Ca^{2+}]_i$ were determined in the acutely isolated SMG physiologic units adhered to 96-well black walled plates (Costar, Tewksbury, MA), using a Flexstation 3 (Molecular Devices) multi-mode microplate reader. The units were loaded with Fura 2-AM and assays were carried out at 37 °C. Basal emission ratios with excitation wavelengths of 340 nm and 380 nm were measured and changes in dye emission ratio determined over 40 seconds after compound addition.

2.8 Statistical analysis

Results were shown as mean ± SD. For multiple comparisons, one-way ANOVA with Sidak's (selected pairs) pairwise tests were used. The calculations were performed with the statistical software package GraphPad Prism (version 7). P values ≤ 0.05 were considered statistically significant.

3. Results

3.1 iNOS upregulation and peroxynitrite formation are early responses following innate immune stimulation.

Western blot was conducted to investigate the expression of iNOS in the control and poly (I:C)-injected submandibular glands (SMGs). Results revealed that poly (I:C) induced upregulation of the iNOS protein (Fig. 1a), which was intensely expressed in the acinar cells, as early as 4 hrs post poly (I:C) administration (Fig. 1b). Peroxynitrite reacts with tyrosine residues in proteins, leading to the formation of stable 3-nitrotyrosine (3-NT), which can be detected by immunohistochemistry [21]. Microscopic examination of the stained sections showed remarkable upregulation of 3-NT following poly (I:C)-injection with more intense staining noted near the basal surfaces of acinar cells (Fig. 1c).

3.2 Extensive acinar iNOS upregulation triggered SMG dysfunction.

It was important subsequently to investigate if iNOS/ONOO- have compromised the secretory machinery in the acutely infected glands. Short (9h) and long-term (24h) inhibitions of iNOS using AG, protected the SMG functions from the poly (I:C) induced secretory dysfunction (Fig. 2a).

3.3 Peroxynitrite-induced nitration of SMG proteins.

To investigate the nitration of SMG proteins with peroxynitrite, western blot analysis was conducted. Tissue lysates of glands injected with the vehicle and poly (I:C) in presence or absence of AG were probed with an antibody to 3-NT. Results revealed excessive nitration of gland proteins, 9h following exposure to a single poly (I:C) dose. In contrast, AG suppressed the peroxynitrite stress signal and the pattern and extent of 3-NT expression returned to near control levels (Fig. 2b).

3.4 Sarcoplasmic/endoplasmic reticulum calcium ATPase (SERCA2b) co-localization with 3-Nitrotyrosine.

Peroxynitrite can severely damage the key regulator of cytosolic Ca^{2+} SERCA [22], which constitutively replenishes the endoplasmic reticulum (ER) Ca^{2+} stores [23]. To explore if the abundantly expressed 3-NT co-localized with SERCA2b, immunohistochemistry was performed. Confocal microscopy displayed the co-labelling of parenchymal cells with antibodies to 3-NT and SERCA2b, 9h after poly (I:C) retrograde injection. Following AG treatment, the iNOS inhibitor succeeded in blocking ONOO- formation and 3-NT co-localization with the calcium pump (Fig. 3a).

3.5 Altered expression of SERCA2b in the SMGs in response to innate immune challenge.

Immunolocalization confirmed distinct distribution of the SERCA2b isoform within the SMG parenchymal cells. In the normal SMGs, the granular cytoplasmic SERCA2b was ubiquitously expressed in every cell type (all ductal and acinar cells). In contrast, the poly (I:C)-injected glands revealed an extremely significant ($p<0.0001$) downregulation of SERCA2b expression, 9h following exposure to the innate immune stimulant. In the infected glands, SERCA2b expression was barely detectable in the acinar cells, with a patchy labelling pattern exhibited in the duct cells. Intriguingly, AG efficiently protected SERCA2b from the poly (I:C) deteriorating effect and maintained it at a level comparable to the control glands (Fig. 3b).

3.6 iNOS-mediated disruption of calcium homeostasis.

It was hypothesized that co-localization of nitrotyrosine with SERCA2b might result in inhibition of the latter. In order to test the hypothesis, carbachol stimulated Ca^{2+} release from the ER, basal cytosolic calcium and calcium levels in the intracellular stores in AG-treated and non-treated SMGs were measured. A novel protocol was optimized and implemented whereby changes of Ca^{2+} release from the ER was recorded using the muscarinic receptor agonist carbachol [20]. Fura-2 ratio (340/380) of fluorescence versus time was monitored for 60 seconds. Experiments conducted revealed that addition of carbachol [50µM] to the vehicle-injected SMG acinar units resulted in prompt $[Ca^{2+}]_i$ mobilization from intracellular ER stores, that was reflected as a sharp

signal increase, followed by a plateau phase. In the poly (I:C) treated glands, an overall decrease in the amplitude of $[Ca^{2+}]_i$ release from the ER was detected, despite the supraphysiologic carbachol dose used. On the contrary, efficient preservation of the intracytoplasmic calcium $[Ca^{2+}]_i$ levels was noted in the glands from AG treated animals, of suggesting that extensive iNOS upregulation had detrimental consequences for acinar calcium homeostasis (Fig. 4a and 4b). To investigate whether iNOS mediated a reduced carbachol response via depleting intracellular stores, we assessed the amount of $[Ca^{2+}]_{ER}$ using ionomycin (an ionophore that, in the absence of external Ca^{2+}, releases Ca^{2+} from the ER in a receptor-independent manner [24; 25]. These experiments demonstrated that in the calcium-free buffer, Ca^{2+} release from intracellular stores induced by ionomycin was significantly decreased in the poly (I:C) injected glands and that the AG-mediated conservation of the carbachol-stimulated calcium release, paralleled a relatively maintained $[Ca^{2+}]_{ER}$ level (Fig. 4c). The Flexstation™ further permitted recording of the baseline calcium, prior to compound addition, which surprisingly revealed an extremely significant increase in Fura-2 340/380 ratio in the poly (I:C) injected glands compared to the control group.

In order to dually assess the impact of extracellular calcium and iNOS inhibition on resting calcium levels in the control and poly (I:C) injected glands, two sets of experiments were conducted, whereby the physiologic units were distinctly incubated in two buffers, one containing 1M EGTA to chelate calcium and the other was EGTA-free and contained $CaCl_2$. Baseline recording of calcium revealed some interesting findings that can be summarized as follows: (i) removal of calcium from the buffer and addition of a chelator, did not change baseline calcium levels in all the **vehicle-injected control** glands of the tested groups. In the ***poly (I:C)-injected group*** (ii) the extremely significant increase ($p<0.0001$) in baseline calcium of the poly (I:C) injected glands (52% more than the vehicle-injected control glands), was extremely reduced ($p<0.00001$) when calcium was removed from the incubation buffer. (iii) Even in the absence of extracellular calcium, acinar units of the poly (I:C) injected glands showed an extremely significant increase in basal calcium compared to the vehicle injected control ($p=0.0004$). In the ***AG-treated group***: (iv) although poly (I:C) still induced an extremely significant increase in basal calcium ($p<0.0001$), the percentage increase represented only 13%, compared to the contralateral vehicle-injected control gland. (v) when the physiologic units were incubated in a calcium-free buffer, the resting $[Ca^{2+}]_i$ nearly paralleled the reference levels recorded in the control gland (Fig. 4d).

3.7 AG inhibited lysosomal discharge

The persistent increase in baseline $[Ca^{2+}]_i$ in the poly (I:C)-injected glands despite calcium removal from the extracellular medium, directed us towards assuming leakage of an intracellular Ca^{2+}-rich organelle. Lysosomes

contain up to 600 mM calcium [26; 27], nearly matching the concentration described for ER, the classic calcium storage organelle [28]. To assess whether poly (I:C) induced lysosomal membrane breach and consequential release of the organelle contents, we assessed the basal immunoexpression of the lysosomal protease cathepsin-B, in the control SMGs, following poly (I:C) injection and treatment with AG-. In the control vehicle injected glands, cathepsin B was exclusively seen in the perinuclear regions of the SMG duct cells. Following intraductal infusion of poly (I:C), cathepsin B was depleted from the peri-nuclear, ductal confinement and showed faint, widespread immunostaining. In contrast, in response to AG priming, the SMGs showed maintained efficient preservation of lysosomal membrane integrity and perinuclear Cathepsin B immunolocalization (Fig. 5).

4. Discussion

In the current study, the physiological responses of the mouse SMG to acute induction of nitrosative stress signals were comprehensively characterized. iNOS upregulation and ONOO- overproduction, which were prompted following innate immune activation of the SGs, impaired saliva secretion via dysregulation of Ca^{2+} homeostasis (Fig. 6). One important finding in the present study, is the demonstrated ability of SG epithelial cells to overexpress iNOS and the reactive nitrogen species ONOO-. By expressing these mediators as early as 4 to 6h after injection of an inflammagen, the parenchymal cells clearly demonstrate their central role in releasing the first inflammatory signals in response to extraneous injuries, independent of the bystander role assigned to infiltrating immune cells [17].

To investigate the injurious role played by iNOS/ONOO- in innate immune-mediated hyposalivation, mice were systemically pre-treated with aminoguanidine hydrochloride, a selective iNOS inhibitor [29; 30]. Since pilot experiments revealed that a single i.p. dose of AG was only sufficient to inhibit iNOS for up to 9h post poly (I:C) retrograde injection, we employed a longer-term inhibition protocol to acquire sufficient iNOS retraction, 24h post poly (I:C) introduction [18], which was mandatory to conduct the calcium experiments. Functional analysis of the AG-treated model revealed remarkable recovery of the poly (I:C) injected glands, at 9h and 24h post infection, compared to the non-treated animals.

Peroxynitrite is believed to be responsible for the harmful effects of iNOS-derived NO during inflammation [31]. It is a powerful oxidant formed *in vivo*, that can directly react with different biomolecules [32]. An important aspect of peroxynitrite-mediated toxicity is its capability of promoting tyrosine nitration in proteins (substitution of a hydrogen by a nitro group ($-NO_2$) in the position 3 of the phenolic ring), with 3-NT being the end product [33]. Indeed, protein 3-NT is established as a biomarker of oxidative stress *in vivo*, being revealed

as a strong biomarker and predictor of disease onset and progression [32]. We showed that decreased nitration of the SMG proteins and retracted 3-NT expression was accompanied by improved SG function. The reduced expression of 3-NT in response to iNOS inhibition is in accordance with the previous demonstration that production of reactive nitrogen species in mice is completely dependent upon NO derived from iNOS [34].

SERCA exists as three isoforms: SERCA2a, SERCA2b and SERCA 3 [35]. While SERCA2a is mainly expressed in excitable cells and smooth muscles, SERCA2b is preferentially localized in the ER of non-excitable cells [36]. SERCA2b, which has been shown to be present in salivary gland cells [37], plays a major role in the rate-limiting replenishing of intracellular calcium stores after secretagouge-stimulated calcium release [38; 39; 40; 41]. The present model revealed acute reduction in SERCA2b expression in the submandibular gland following local treatment with poly (I:C). Previous studies have shown NO-mediated downregulation of SERCA2b expression [42], presumably through interfering with binding of transcription factors to the SERCA2 promoter [12]. In addition, the poly (I:C)-injected glands exhibited extensive co-localization of 3-NT and SERCA2b. Given the observed decrease in SERCA2b expression and its vicinity to a potent oxidant, it was surmised that would be a reduction in SERCA2b activity, and loss of its tight control on ER and cytosolic calcium levels. Our hypothesis was validated by the dramatic changes in acinar Ca^{2+} signalling measured 24h after poly (I:C) introduction. Disruptions were in the form of reduced release of Ca^{2+} from the ER, evoked by either carbachol or ionomycin in Ca^{2+}-free medium, as well as elevated resting $[Ca^{2+}]_i$ levels prior to compound applications.

The reduction in magnitude of Ca^{2+} release from the ER independent of activation of IP3R; i.e. with ionomycin, suggested that $[Ca^{2+}]_{ER}$ content was diminished and this was reflected in the impairment of carbachol-stimulated Ca^{2+} release. The reduced expression and physical co-localization of SERCA2b and peroxynitrite may explain the inability of the pump to replenish $[Ca^{2+}]_{ER}$, accounting for the reduced Ca^{2+} content in the intracellular store. Importantly, the prevention of ONOO- accumulation by AG, preserved the calcium response to carbachol and ionomycin stimulation, which highlights the involvement of upregulated iNOS and peroxynitrite in the impairment of acinar cells following innate immune challenge. Future experiments to verify the inhibition of SERCA2b and other calcium pumps and channels in response to excessive iNOS production can provide valuable insights into the mechanisms of SG dysfunction associated with disrupted redox status in response to proinflammatory stimuli. Resting $[Ca^{2+}]_i$ showed an extremely significant elevation in the poly (I:C)-injected glands, prior to secretagogue stimulation. Removal of calcium from the extracellular buffer as well as treatment of the mice with AG, remarkably retrieved the basal $[Ca^{2+}]_i$ levels, suggesting that iNOS mediated a breach of

the plasma membranes in the poly (I:C) injected SMGs. Interestingly, in the current model, immunohistochemical staining revealed the preferential localization of 3-NT in the acinar and duct cell membranes, which may suggesting that peroxynitrite-induced damage of plasma membranes would occur resulting in loss of cellular Ca^{2+} [43; 44] and sequential changes in membrane permeability and fluidity [45]. Despite removal of Ca^{2+} from the prepared buffers, the baseline calcium level was not completely restored in the poly (I:C) injected glands, which suggested leakage from an intracellular source. Immunostaining of the tissue sections from poly (I:C) injected SMGs verified lysosomal membrane permeabilization (LMP) and the consequent release of cathepsin B, the most abundant protease [46]. Interestingly, cathepsin B may constitute an amplifying feedback loop, in which a small amount of released cathepsin B triggers more extensive LMP from outside the lysosome [47; 48]. Several mechanisms can disrupt the integrity of the lysosomal membrane [49]. The exact trigger for disruption of lysosomes in the current model has not been comprehensively investigated but the rapid involvement of iNOS-dependant mechanisms has been verified. Further studies will be conducted to investigate the pathological consequences of cathepsin B release, given its capability to proteolytically modify molecules implicated in cell death pathways [49].

Acute depletion of $[Ca^{2+}]_{ER}$ is an upstream prerequisite in the pathophysiology of many diseases [50]. The present study has identified iNOS as a key mediator that disrupts acinar cell calcium signalling leading to impaired exocrine secretion following activation of innate immunity in an acute salivary gland injury model.

Acknowledgements

We acknowledge Dr Araz Ahmed (Craniofacial Development & Stem Cell Biology, King's College London) for his support with the confocal imaging and Dr David Andersson (Wolfson Centre for Age Related Diseases, King's College London) for his support with the Flexstation™ settings.

Conflict of interest

The authors declare no conflict of interest.

Funding

This research did not receive any specific grant from funding agencies in the public, commercial, or not-for-profit sectors.

References

[1] G.B. Proctor, The physiology of salivary secretion, Periodontology 2000 70 (2016) 11-25.

[2] G.B. Proctor, G.H. Carpenter, Salivary secretion: mechanism and neural regulation, Monogr Oral Sci 24 (2014) 14-29.

[3] I.S. Ambudkar, Calcium signalling in salivary gland physiology and dysfunction, The Journal of Physiology 594 (2016) 2813-2824.

[4] A.V. Tepikin, S.G. Voronina, D.V. Gallacher, O.H. Petersen, Pulsatile Ca2+ extrusion from single pancreatic acinar cells during receptor-activated cytosolic Ca2+ spiking, J Biol Chem 267 (1992) 14073-6.

[5] H. Mogami, A.V. Tepikin, O.H. Petersen, Termination of cytosolic Ca2+ signals: Ca2+ reuptake into intracellular stores is regulated by the free Ca2+ concentration in the store lumen, EMBO J 17 (1998) 435-42.

[6] X. Liu, I.S. Ambudkar, Characteristics of a store-operated calcium-permeable channel: sarcoendoplasmic reticulum calcium pump function controls channel gating, J Biol Chem 276 (2001) 29891-8.

[7] N. Holdgate, E.W. St Clair, Recent advances in primary Sjogren's syndrome, F1000Res 5 (2016).

[8] J. Kiripolsky, L.G. McCabe, J.M. Kramer, Innate immunity in Sjogren's syndrome, Clin Immunol 182 (2017) 4-13.

[9] L.Y. Teos, Y. Zhang, A.P. Cotrim, W. Swaim, J.H. Won, J. Ambrus, L. Shen, L. Bebris, M. Grisius, S.I. Jang, D.I. Yule, I.S. Ambudkar, I. Alevizos, IP3R deficit underlies loss of salivary fluid secretion in Sjogren's Syndrome, Sci Rep 5 (2015) 13953.

[10] E.U. Uehara, S. Shida Bde, C.A. de Brito, Role of nitric oxide in immune responses against viruses: beyond microbicidal activity, Inflamm Res 64 (2015) 845-52.

[11] D. Salvemini, H. Ischiropoulos, S. Cuzzocrea, Roles of nitric oxide and superoxide in inflammation, Methods Mol Biol 225 (2003) 291-303.

[12] P. Pacher, J.S. Beckman, L. Liaudet, Nitric oxide and peroxynitrite in health and disease, Physiol Rev 87 (2007) 315-424.

[13] T. Hayashi, Dysfunction of lacrimal and salivary glands in Sjogren's syndrome: nonimmunologic injury in preinflammatory phase and mouse model, J Biomed Biotechnol 2011 (2011) 407031.

[14] N. Hanaue, I. Takeda, Y. Kizu, M. Tonogi, G.Y. Yamane, Peroxynitrite formation in radiation-induced salivary gland dysfunction in mice, Biomed Res 28 (2007) 147-51.

[15] A. Shaalan, G. Carpenter, G. Proctor, Caspases are key regulators of inflammatory and innate immune responses mediated by TLR3 in vivo, Molecular Immunology 94 (2018) 190-199.

[16] Y.S. Cheng, X.D. Cong, D.Z. Dai, Y. Zhang, Y. Dai, Argirein alleviates corpus cavernosum dysfunction by suppressing pro-inflammatory factors p66Shc and ER stress chaperone Bip in diabetic rats, J Pharm Pharmacol 65 (2013) 94-101.

[17] A. Shaalan, G. Carpenter, G. Proctor, Epithelial disruptions, but not immune cell invasion, induced secretory dysfunction following innate immune activation in a novel model of acute salivary gland injury, J Oral Pathol Med (2017).

[18] A.S. MacFarlane, M.G. Schwacha, T.K. Eisenstein, In vivo blockage of nitric oxide with aminoguanidine inhibits immunosuppression induced by an attenuated strain of Salmonella typhimurium, potentiates Salmonella infection, and inhibits macrophage and polymorphonuclear leukocyte influx into the spleen, Infect Immun 67 (1999) 891-8.

[19] C.A. Schneider, W.S. Rasband, K.W. Eliceiri, NIH Image to ImageJ: 25 years of image analysis, Nat Methods 9 (2012) 671-5.

[20] A.K. Shaalan, G. Carpenter, G. Proctor, Measurement of intracellular calcium of submandibular glands using a high throughput plate reader, Journal of Biological Methods; Vol 4, No 3 (2017) (2017).

[21] F. Giannessi, F. Ursino, B. Fattori, M.A. Giambelluca, M.C. Scavuzzo, A. Nacci, F. Fornai, R. Ruffoli, Expression of 3-nitrotyrosine, a marker for peroxynitrite, in nasal polyps of nonatopic patients, Med Sci Monit 16 (2010) CR172-179.
[22] C.M. Misquitta, D.P. Mack, A.K. Grover, Sarco/endoplasmic reticulum Ca2+ (SERCA)-pumps: link to heart beats and calcium waves, Cell Calcium 25 (1999) 277-90.
[23] I.S. Ambudkar, Ca(2)(+) signaling and regulation of fluid secretion in salivary gland acinar cells, Cell Calcium 55 (2014) 297-305.
[24] P.R. Albert, A.H. Tashjian, Jr., Ionomycin acts as an ionophore to release TRH-regulated Ca2+ stores from GH4C1 cells, Am J Physiol 251 (1986) C887-91.
[25] J.B. Smith, T. Zheng, R.M. Lyu, Ionomycin releases calcium from the sarcoplasmic reticulum and activates Na+/Ca2+ exchange in vascular smooth muscle cells, Cell Calcium 10 (1989) 125-34.
[26] K.A. Christensen, J.T. Myers, J.A. Swanson, pH-dependent regulation of lysosomal calcium in macrophages, J Cell Sci 115 (2002) 599-607.
[27] E. Lloyd-Evans, A.J. Morgan, X. He, D.A. Smith, E. Elliot-Smith, D.J. Sillence, G.C. Churchill, E.H. Schuchman, A. Galione, F.M. Platt, Niemann-Pick disease type C1 is a sphingosine storage disease that causes deregulation of lysosomal calcium, Nat Med 14 (2008) 1247-55.
[28] F.L. Bygrave, A. Benedetti, What is the concentration of calcium ions in the endoplasmic reticulum?, Cell Calcium 19 (1996) 547-51.
[29] W.R. Waz, J.B. Van Liew, L.G. Feld, Nitric oxide-inhibitory effect of aminoguanidine on renal function in rats, Kidney Blood Press Res 20 (1997) 211-7.
[30] F. Viaro, F. Nobre, P.R. Evora, Expression of nitric oxide synthases in the pathophysiology of cardiovascular diseases, Arq Bras Cardiol 74 (2000) 380-93.
[31] S. Aydogan, M.B. Yerer, A. Goktas, Melatonin and nitric oxide, J Endocrinol Invest 29 (2006) 281-7.
[32] S. Bartesaghi, R. Radi, Fundamentals on the biochemistry of peroxynitrite and protein tyrosine nitration, Redox Biology 14 (2018) 618-625.
[33] D.J. Bigelow, Nitrotyrosine-modified SERCA2: a cellular sensor of reactive nitrogen species, Pflugers Arch 457 (2009) 701-10.
[34] A. Koarai, M. Ichinose, H. Sugiura, M. Tomaki, M. Watanabe, S. Yamagata, Y. Komaki, K. Shirato, T. Hattori, iNOS depletion completely diminishes reactive nitrogen-species formation after an allergic response, Eur Respir J 20 (2002) 609-16.
[35] K.D. Wu, W.S. Lee, J. Wey, D. Bungard, J. Lytton, Localization and quantification of endoplasmic reticulum Ca(2+)-ATPase isoform transcripts, Am J Physiol 269 (1995) C775-84.
[36] I.S. Ambudkar, Regulation of calcium in salivary gland secretion, Crit Rev Oral Biol Med 11 (2000) 4-25.
[37] M.G. Lee, X. Xu, W. Zeng, J. Diaz, R.J. Wojcikiewicz, T.H. Kuo, F. Wuytack, L. Racymaekers, S. Muallem, Polarized expression of Ca2+ channels in pancreatic and salivary gland cells. Correlation with initiation and propagation of [Ca2+]i waves, J Biol Chem 272 (1997) 15765-70.
[38] M.J. Berridge, P. Lipp, M.D. Bootman, The versatility and universality of calcium signalling, Nat Rev Mol Cell Biol 1 (2000) 11-21.
[39] D.M. Bers, Cardiac excitation-contraction coupling, Nature 415 (2002) 198-205.
[40] V. Homann, E. Kinne-Saffran, W.H. Arnold, P. Gaengler, R.K. Kinne, Calcium transport in human salivary glands: a proposed model of calcium secretion into saliva, Histochem Cell Biol 125 (2006) 583-91.
[41] P. Vangheluwe, L. Raeymaekers, L. Dode, F. Wuytack, Modulating sarco(endo)plasmic reticulum Ca2+ ATPase 2 (SERCA2) activity: cell biological implications, Cell Calcium 38 (2005) 291-302.
[42] A.K. Cardozo, F. Ortis, J. Storling, Y.M. Feng, J. Rasschaert, M. Tonnesen, F. Van Eylen, T. Mandrup-Poulsen, A. Herchuelz, D.L. Eizirik, Cytokines downregulate the sarcoendoplasmic reticulum pump Ca2+ ATPase 2b and deplete endoplasmic

reticulum Ca2+, leading to induction of endoplasmic reticulum stress in pancreatic beta-cells, Diabetes 54 (2005) 452-61.
[43] N. Hogg, B. Kalyanaraman, Nitric oxide and lipid peroxidation, Biochim Biophys Acta 1411 (1999) 378-84.
[44] R. Radi, J.S. Beckman, K.M. Bush, B.A. Freeman, Peroxynitrite-induced membrane lipid peroxidation: the cytotoxic potential of superoxide and nitric oxide, Arch Biochem Biophys 288 (1991) 481-7.
[45] C. Richter, Biophysical consequences of lipid peroxidation in membranes, Chem Phys Lipids 44 (1987) 175-89.
[46] A. Rossi, Q. Deveraux, B. Turk, A. Sali, Comprehensive search for cysteine cathepsins in the human genome, Biol Chem 385 (2004) 363-72.
[47] A.-C. Johansson, H. Appelqvist, C. Nilsson, K. Kågedal, K. Roberg, K. Öllinger, Regulation of apoptosis-associated lysosomal membrane permeabilization, Apoptosis 15 (2010) 527-540.
[48] N. Liu, S.M. Raja, F. Zazzeroni, S.S. Metkar, R. Shah, M. Zhang, Y. Wang, D. Bromme, W.A. Russin, J.C. Lee, M.E. Peter, C.J. Froelich, G. Franzoso, P.G. Ashton-Rickardt, NF-kappaB protects from the lysosomal pathway of cell death, Embo j 22 (2003) 5313-22.
[49] A. Serrano-Puebla, P. Boya, Lysosomal membrane permeabilization in cell death: new evidence and implications for health and disease, Ann N Y Acad Sci 1371 (2016) 30-44.
[50] D. Mekahli, G. Bultynck, J.B. Parys, H. De Smedt, L. Missiaen, Endoplasmic-reticulum calcium depletion and disease, Cold Spring Harb Perspect Biol 3 (2011).

Tables

Table 1. List of antibodies used in immunohistochemical and western blot analysis

Antibody	Source & Catalogue Number	Host	Working Dilution
iNOS	Novus Biologicals, USA, NB300-605	Rabbit	1:1000
3-Nitrotyrosine	Millipore, 05-233	Mouse	1:1000
SERCA2 ATPase	Novus Biologicals, NBP2-20305	Rabbit	1:1000
Cathepsin B (S-12)	Santa Cruz Biotechnology, sc-6493	Goat	1:1000
Polyclonal Goat Anti-Rabbit Immunoglobulins-HRP	Dako, P0448	Goat	1:200
Polyclonal Goat Anti-Mouse Immunoglobulins- HRP	Dako, P0447	Goat	1:100
Goat anti-Mouse IgG (H+L) Secondary Antibody, Alexa Fluor® 594 conjugate	Thermo Fisher Scientific, A-11005	Goat	1:1000
Donkey anti-Rabbit IgG (H+L) Secondary Antibody, Alexa Fluor 488	Thermo Fisher Scientific, A-21206	Donkey	1:1000

Figure Legends:

Figure 1: iNOS and Peroxynitrite expression in the SMGs. A: Western blot analysis of the upregulated protein levels of iNOS, in response to poly (I:C) injection (P-PIC), compared to the control, vehicle-injected group (V-C). The data are representative of results from three independent experiments. **B:** Photomicrographs showing negative expression of iNOS in the vehicle injected SMGs, compared to the early and intense immunolabelling of acini (yellow outlines) following poly (I:C). **C:** Upregulated expression of the peroxynitrite marker 3-nitrotyrosine (3-NT) was noted in the ducts (red outline) as well as the basal surfaces of acinar cells (black arrows) following poly (I:C). Original magnification=40x.

Figure 2: Salivary gland function and peroxynitrite activity. A: Functional analysis following poly (I:C) and the selective iNOS inhibitor, aminoguanidine. Enhancement of SMG secretory function from mice treated with aminoguanidine (AG+PIC), compared to glands from mice which received poly (I:C) only (PIC). Minimum n=3 mice per group, maximum n=6. **B: Western blot of the peroxynitrite marker; 3-Nitrotyrosine.** Poly (I:C) prompted nitroxidative stress in the SMGs following poly (I:C) introduction (9h P-PIC): a plethora of SMG proteins exhibited tyrosine nitration compared to the control (V-C), which was markedly reduced upon aminoguanidine treatment (AG+9h P-PIC). Representative data from three independent experiments.

Figure 3: Immunohistochemistry of SERCA2 ATPase and peroxynitrite activity. A: Microphotographs of multi-colour confocal microscopy analysis confirming co-localized expression of SERCA2 ATPase and 3-NT and. In the ***normal SMGs***, negative 3-NT expression and intense ductal and mild acinar clustering of the SERCA2. ***9h Post infection with poly (I:C)***, abundant co-localization of the upregulated 3-NT staining with down-regulated SERCA2 staining. ***AG-treated SMGs*** revealed the obvious decline of 3-NT expression and the regular SERCA2 labelling of the SMG cells. **B: Immunohistochemistry and digital image analysis of SERCA2b ATPase in the control and poly (I:C)-injected glands from the AG treated and non-treated mice.** In the control glands, SERCA2 was intensely immunoexpressed in the basal domains of striated ducts, as well as in the form of peri-nuclear cytoplasmic granules in the acinar cells. After poly (I:C) retrograde infusion, an overall retraction in the SERCA2 expression was perceived, which was efficiently reversed when mice were primed with the iNOS inhibitor, aminoguanidine (AG). SERCA2b immunostaining area percentage: *p= 0.0235 and ****p<0.0001. Representative data from three independent experiments.

Figure 4: Changes in intracellular Ca^{2+} in poly (I:C) treated SMGs in response to AG pre-treatment. A and B: Fura-2-detected fluorescent signals in SMGs, in response to stimulation with 50 µM carbachol. SMGs from mice treated or not treated with AG as well as the relevant vehicle injected controls were used. The cholinergic agonist carbachol was added to detect the $[Ca^{2+}]_i$ response in the acinar units. Stimulated Ca^{2+} response graph represents the Δ340/380 (maximal $[Ca^{2+}]_i$ increase after carbachol application minus its basal expression prior to stimulation). Poly (I:C) triggered 91% reduction in the $[Ca^{2+}]_i$, which was reduced to only 13% in the glands from AG-treated animals, compared to the glands which received the vehicle only. **C: Ionomycin-induced Ca^{2+} release from the intracellular stores.** Isolated acinar cells of vehicle and poly (I:C) injected SMGs from AG treated and non-treated animals were incubated in Ca-free medium. Poly (I:C) reduced ionomycin-stimulated Ca^{2+} release from the internal stores by 70%, whereas in the presence of AG, only 36% reduction was perceived. **D: Baseline 340/380 ratio in the SMGs treated or not treated with AG.** Differential changes in baseline calcium among the tested physiologic units as explained in the text. Ca: Calcium-containing buffer, NCa: Incubation buffer free of CaCl2 and containing 1M EGTA.

Figure 5: Cathepsin B immunoexpression in the SMGs. Photomicrographs showing the characteristic fine perinuclear granules of cathepsin B in the control SMG ducts, consistent with its lysosomal localization. 24h post its intraductal infusion (24h P-PIC), poly (I:C) induced extra-lysosomal cathepsin B release into the SMG tissues. AG treatment (AG+24h P-PIC) caused the efficient retention of the peri-nuclear lysosomal protease in the ducts of the infected glands, similar to its immunolocalization in the control tissues. Original magnification= 40x.

Figure 6: Illustration summarising the impact of innate immune-mediated iNOS overexpression on the exocrine salivary gland secretory machinery. Parenchyma-expressed iNOS/ONOO- disrupted the expression and possibly the activity of the SERCA2b, which tightly controls the cytoplasmic as well as the endoplasmic reticulum calcium levels. Physiological saliva production is entirely dependent on the integrity of intracellular calcium signalling, the interruption of which interfered with the ability of the submandibular glands to secrete normally.

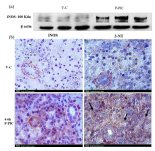

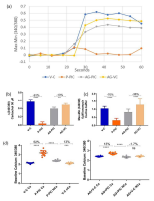

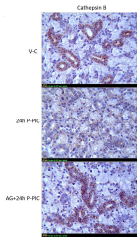

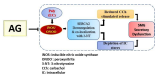

(a)

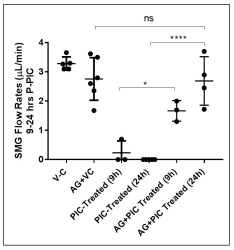

(b)

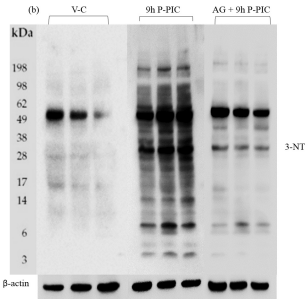

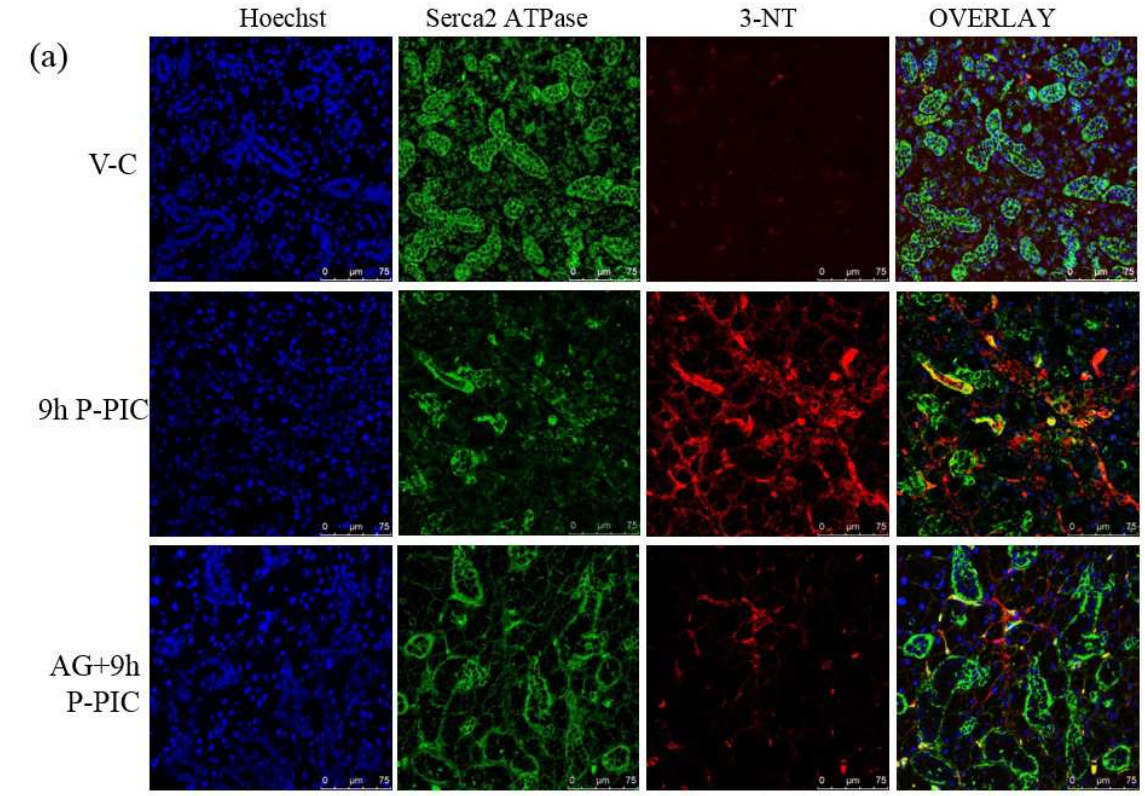
(a)
Hoechst
Serca2 ATPase
3-NT
OVERLAY
V-C
9h P-PIC
AG+9h P-PIC

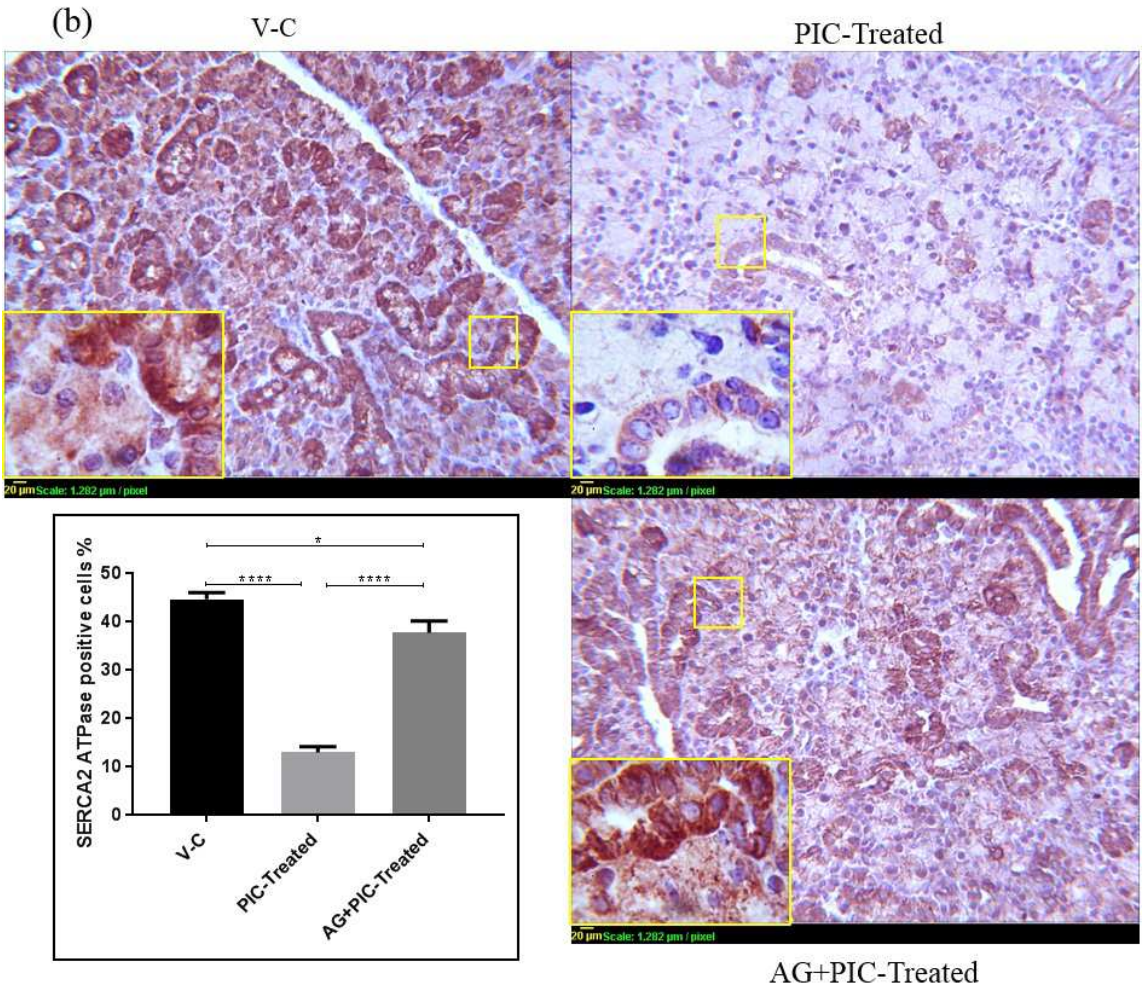
(b)
V-C
PIC-Treated
AG+PIC-Treated
SERCA2 ATPase positive cells %
50
40
30
20
10
0
*
****
****
V-C
PIC-Treated
AG+PIC-Treated

Highlights

- Innate immune stimulant poly (I:C) induced prompted the upregulated expression of iNOS and 3-Nitrotyrosine in the C57BL/6 submandibular glands.
- Aminoguanidine, a selective iNOS inhibitor blocked the nitrosative signal *in vivo* and protected the SMG secretory machinery.
- iNOS/peroxynitrite interfered with the SMG secretory ability via dysregulating the expression of SERCA2b and perturbing calcium homeostasis.